Clinical Biomechanics 36 (2016) 46–51

Contents lists available at ScienceDirect

Clinical Biomechanics

journal homepage: www.elsevier.com/locate/clinbiomech

Prediction of stemless humeral implant micromotion during upper limb activities

Philippe Favre [a,*], Adam D. Henderson [a]

[a] Zimmer Biomet, Sulzerallee 8, 8404 Winterthur, Switzerland

ARTICLE INFO

Article history:
Received 4 March 2016
Received in revised form 29 April 2016
Accepted 5 May 2016

Keywords:
Primary stability
Micromotion
Stemless shoulder
Finite element
Physiologic loading

ABSTRACT

Background: Adequate primary stability is essential for the long term success of uncemented stemless shoulder implants. The goal of this study was to evaluate the micromotion of a stemless humeral implant during various upper limb activities.
Methods: A finite element model was validated by reproducing experimental primary stability testing. Loading from an instrumented prosthesis representing a set of 29 upper limb activities were applied within the validated FE model. Peak micromotion and percentage area for different micromotion thresholds were considered.
Findings: In all simulated activities, at least 99% of the implant surface experienced micromotion below 150 μm. Micromotion depended strongly on loading with large discrepancies between upper limb activities. Carrying no external weight and keeping the arm at lower angles induced lower micromotion. Activities representative of demanding manual labor generally led to higher micromotion. Axilla crutches led to lower micromotion than forearm crutches. Micromotion increased when a wheelchair was used on slopes above 2% inclination.
Interpretation: Micromotions below the 150 μm threshold below which bone ingrowth occurs were measured over at least 99% of the implant surface for all simulated activities. Peak micromotion dependence on activity type demonstrates the need to consider physiologic in vivo loading and the full contact interface in primary stability evaluations. Focusing on activities with no hand weight and low arm motions during the rehabilitation period may enhance primary stability. For patients unable to walk without aids, axilla crutches and motorized wheelchairs might be more beneficial than forearm crutches and manual drive wheelchairs respectively.

1. Introduction

Fixation of prostheses to the humerus has traditionally been achieved by means of a cemented or uncemented stem inserted into the humeral canal. Recently, humeral stemless implants have been developed to reduce potential complications associated with the stem (Berth and Pap, 2013; Churchill, 2014; Habermeyer P et al., 2015): the reconstruction of the natural humeral head anatomy is improved in the absence of positioning constraints with respect to the humeral shaft; the risk of peri-prosthetic fractures is eliminated and the surgical technique is simplified; more bone stock is preserved for potential later revisions representing a significant advantage in younger patients; finally, these implants are typically indicated for cementless use in order to further enhance bone preservation and reduce the difficulties associated with cement extraction during revision.

The long term success of uncemented stemless shoulder implants relies on osseointegration, which can only be achieved with adequate primary stability. Nevertheless, very little knowledge on the primary stability of cementless stemless implants is available. The major reasons are that stemless prostheses have been introduced to the clinic fairly recently (Churchill, 2014) and radiological assessment of their primary stability can be more challenging than for cemented stems (Razmjou et al., 2013). In addition, knowledge from primary stability of stemmed implants cannot be directly transferred to stemless implants. First, fixation length is much shorter in a stemless implant creating a much smaller available lever to resist external moments. Second, the anchor of a stemless implant interacts with cancellous bone whereas cementless stemmed implants rely on support of the much stiffer cortical bone. Bone quality and load magnitude have been shown to significantly influence stemless implant micromotion in an in vitro study, while anchor size did not significantly affect initial stability (Favre et al., 2016). Due to the experimental nature of these tests, simplified loading conditions were implemented and micromotion was assessed in specific interface locations. Loads acting at the shoulder are complex and versatile due to the variable nature of upper limb activities. In order to more closely evaluate the daily fixation demands of a cementless implant, it would be essential to evaluate the influence of more realistic loading conditions (Berth et al., 2016) and assess the micromotion distribution on the full bone-implant interface.

* Corresponding author: Philippe Favre Sulzerallee 8, CH-8404 Winterthur, Switzerland.
E-mail addresses: philippe.favre@zimmerbiomet.com (P. Favre), adam.henderson@zimmerbiomet.com (A.D. Henderson).

http://dx.doi.org/10.1016/j.clinbiomech.2016.05.003
0268-0033/

The purpose of this study was to use a three dimensional (3D) finite element (FE) model of a stemless shoulder implant to 1) evaluate what level of micromotion can be expected during in vivo use before bone ingrowth occurs, 2) compare activities with respect to implant micromotion and 3) provide guidelines on activities that should be preferred or avoided during the rehabilitation period.

2. Methods

A stemless implant (Sidus® Stem-Free Shoulder, Zimmer GmbH, Winterthur, Switzerland) with 4 perpendicular, rough blasted anchorage fins was virtually implanted in a humerus. A previous experimental primary stability test (Favre et al., 2016) was reproduced and the results were compared for model validation. The validated model was then used to study the effect of in vivo loading on micromotion at the bone-implant interface.

2.1. Finite element model

One humerus free of visible deformities (right side of a 69 year old male donor) was selected for the creation of the FE model. This bone was chosen based on the average physical constitution of the donor (76 kg bodyweight and 180 cm tall, 23.3 body mass index) and midrange humeral trabecular bone quality (0.24 g/cm^3) when compared to the range (0.04 to 0.56 g/cm^3) of previously experimentally tested bones (Favre et al., 2016), and because the surgical technique recommends implanting this prosthesis in good bone quality only (Zimmer Inc, 2012). The intact humerus was CT scanned (Toshiba Aquilion, 0.5 mm in plane resolution and 1 mm slice thickness), the 3D surfaces of the cancellous and cortical bone were obtained by segmentation of the CT images and 3D reconstruction was performed in Mimics (Version 14.1, Materialise, Leuven, Belgium). The humeral head was virtually resected (Supplementary Fig. 1) at the height, version and inclination that had been measured in the experiment (Unigraphics, Siemens PLM Software, Plano, TX, USA). The bone was cut with a modified implant model to account for the removed bone in the implant fin windows during the implantation process. The computer aided design model of the Sidus® anchor was virtually implanted, replicating the position and orientation achieved in the experiment. The bone 40 mm distal from the humeral head center was resected to reduce model size. The assembly was exported to ANSYS (Workbench 15.0, Ansys Inc., Canonsburg, PA, USA) for quadratic tetrahedral meshing and FE analysis. A mesh sensitivity analysis was performed on the validation model setup to identify the level of mesh refinement that led to less than 5% change in peak micromotion (Supplementary Fig. 2). The location of peak micromotion was the same for all tested mesh refinements. The final mesh resulted in a model totaling 85,000 elements (24,000 elements for the anchor, 56,000 for the cancellous bone and 5000 for the cortical bone) with 1 mm side length at the bone implant interface. Average generic linear-elastic material properties (Dalstra et al., 1993; Frich and Jensen, 2014; Keller, 1994; Li and Aspden, 1997; Rice et al., 1988) were applied to the cancellous (210 MPa and 0.4 Poisson's ratio) and to the cortical bone (17 GPa and 0.4 Poisson's ratio) to match the average bone density of the tested bone. Isotropic linear-elastic material properties of Ti–6Al–4V were applied to the anchor (114 GPa Young's modulus and 0.34 Poisson's ratio). The press-fit between the bone and the implant was not modeled. Coulomb frictional contacts were defined between the cancellous bone and the rough blasted faces of the anchor with a 0.6 friction coefficient (Biemond et al., 2011; Grant et al., 2007). Contacts between the cancellous bone and the surfaces of the implant that are not rough blasted were set to be frictionless to simulate a worst case condition. The humeral head was not modeled; all forces and moments were applied directly to the anchor morse taper and centered on the origin of the humeral head sphere (Supplementary Fig. 1). The distal resection surface of the bone was fully constrained.

2.2. Comparison of virtual and experimental micromotion results

The experimental test is described in detail in a previously published study (Favre et al., 2016). A stemless shoulder implant size Large (Sidus® Stem-Free Shoulder, Zimmer GmbH, Winterthur, Switzerland) was implanted according to the surgical technique (Zimmer Inc, 2012) with a size 50 × 18 mm Sidus® humeral head. The humerus was cemented (Osteobond® Copolymer Bone Cement, Zimmer, Warsaw, IN) in a specimen holder for fixation to the testing machine. A 820 N load was applied to the humeral head at a 30° angle from the anchor axis in the coronal plane for 100 cycles in force control at 300 N/s using a single axis material testing machine (Zwick 1456, Zwick Roell, Ulm, Germany). One approximately 1 × 1 cm window was created on the side of the bone to image the cancellous bone-implant interface with a high resolution camera system (model Prosilica GX1920, AVT, Stadtroda, Germany) equipped with a telecentric lens (model S5LPJ4425, Sill Optics GmbH & Co, Wendelstein, Germany). Pre-load (50 N) and 820 N load images were compared using Matlab (MathWorks Inc., Natick, MA, USA) and an image analysis subroutine using the software Fiji (Schindelin et al., 2012). The script removed any rotation and translation of the system or the camera to align the two images and identified the same landmarks in both images to evaluate the relative implant–bone motion. Micromotion values for all landmarks within the measurement window were averaged.

The window created in the bone during the experiment for imaging of the bone-implant interface was virtually reproduced for validation of the FE model only and the 820 N force was applied. Micromotion magnitudes (resultant, parallel and perpendicular components to the resection plane) for all nodes in the bone window created for high resolution imaging measurement were averaged and compared with the experimental values (Fig. 1).

2.3. Physiologic loading

After the model was validated, the imaging measurement window was removed from the bone model and physiologic glenohumeral joint resultant forces representative of an extensive set of upper limb activities were applied to evaluate the primary stability of the implant

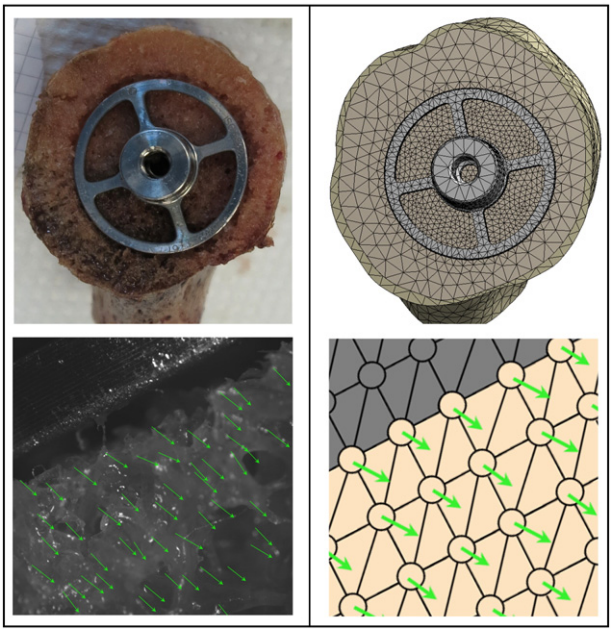

Fig. 1. FE model validation. Experimentally tested bone (top left) and corresponding virtual model (top right). Comparison of experimentally obtained micromotion using high resolution interface imaging (bottom left) to the nodal relative displacement (bottom right).